

# GEOCHEMICAL CHARACTERISTICS AND SUBSURFACE STRUCTURE OF CHANG'E-4 LANDING SITE

X. H. Fu<sup>1</sup>, J. Zhang<sup>1</sup>, L. C. Jia<sup>2</sup>, Z. C. Ling<sup>1</sup>, Y. Z. Jia<sup>2</sup>, Y. L. Zou<sup>2</sup> <sup>1</sup>Shandong Provincial Key Laboratory of Optical Astronomy and Solar-Terrestrial Environment, Institute of Space Sciences, Shandong University ([fuqxh@sdu.edu.cn](mailto:fuqxh@sdu.edu.cn)),

<sup>2</sup>National Space Science Center, Chinese Academy of Sciences.

**Introduction:** On the 3<sup>rd</sup> January, 2019, Chang'E-4 (CE-4) landed on the east of Von Kármán crater (177.6°E and 45.5°S) within South Pole-Aitken basin (SPA). This is the first in-situ exploration mission on lunar farside. In this study, we investigated the geochemical characteristics of this area and its subsurface structure. This could provide geological background for further in-situ data interpretation.

**Geological background:** SPA is a vast, ancient impact structure on the Moon. This unique location is known holding keys to understanding several fundamental questions in lunar and planetary science, such as lunar cataclysm and impact flux in early lunar history, lunar crustal structure and compositional heterogeneity, lunar farside volcanism<sup>[1]</sup>. SPA basin has been proposed as the landing area of several sample return missions, such as MoonRise mission<sup>[2]</sup>.

Using Moon Mineralogy Mapper (M<sup>3</sup>) data, Moriarty et al. (2018) revealed four distinct compositional zones across SPA: SPA Compositional Anomaly (SPACA), Mg-Pyroxene Annulus, Heterogeneous Annulus, and SPA Exterior [3].

Von Kármán crater is a pre-Nectarian crater with the diameter of 186 km. It is located to the south of Leibnitz crater, is joined to the northeast rim of Finsen crater. Attached to the southern rim of Von Kármán is Alder crater. Oresme and Oresme V crater (a thorium hotspot) is located to the west-northwest of Von Kármán. Finsen crater and other complex large craters (Bhabha, Stoney) within SPACA exhibit distinctly Mg-rich pyroxenes in their central peaks, Ca/Fe-rich pyroxene in the walls and floors. Von Kármán and Alder craters both lie in Mg-Pyroxene Annulus and presents extensive Mg-pyroxene bearing materials. Except this, pure plagioclase was found in the eastern mound and southern wall of Alder crater, which is quite rare within SPA<sup>[3]</sup>.

## Geochemistry of CE-4 landing site and regolith

**mixing:** The landing site of CE-4 mission lies on the eastern floor of Von Kármán crater. The floor is mostly covered with mare basalt. Using the Clementine and Lunar prospector data, we found the area shows low FeO (13-18wt%) and TiO<sub>2</sub> (1-3 wt%)<sup>[4]</sup>, but elevated Th (2.0-2.5 ppm)<sup>[5]</sup>. The intermediate FeO and moderate to low Th features fit the criteria for high-Al (HA) mare basalts: FeO = 12-18 wt%, TiO<sub>2</sub> = 1-5 wt%, Th = 0-4 ppm<sup>[6]</sup>. This suggests Von Kármán crater a potential location of HA basalt exposures.

HA basalt are mostly found in the Apollo 14 samples. Apollo 14 landed on the Fra Mauro region,

one of Thorium-rich spots. These basalts are relatively enriched in  $\text{Al}_2\text{O}_3$  (11-16 wt%)<sup>[7]</sup>. HA Basalt fragments are also identified in Luna 16 samples. The Al-rich nature of this type basalt is related with more modal plagioclase in them than other mare basalts. Apollo 14 HA basalt, with the age from 3.9-4.3 Ga, represents mare volcanic activities predates the main mare magmatism in lunar nearside (3.9-3.1 Ga)<sup>[7]</sup>. Luna 16 HA basalts are much younger (~3.4 Ga)<sup>[8]</sup>.

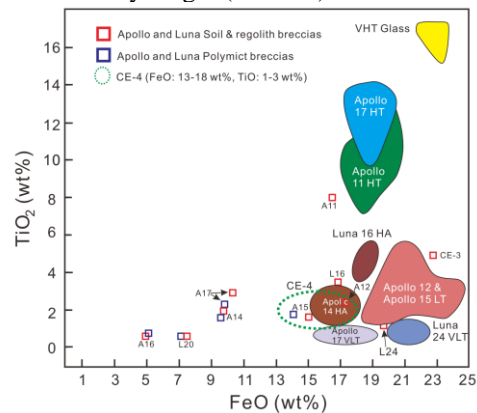


**Figure 1 Variations of FeO and TiO<sub>2</sub> in lunar rock, soil and regolith samples. This diagram is modified from [9]. The data of Apollo and Luna soils and regolith breccias are from [10]. Chang'E-3(CE-3) basalt data are from [11].**

For Von Kármán crater, Huang et al. (2018) determined the absolute model ages of the mare units located within Von Kármán <sup>[12]</sup>. They yielded the Imbrium age (~3.6 Ga) for both whole volcanic floor and CE-4 landing subarea. Mare unit filled Von Kármán floor falls in the major volcanism peak ranging from 3.9-3.1 Ga, being clearly younger than typical Apollo 14 HA basalt. We cannot rule out the presence of HA basalt on the basis of the existing geochemical and chronology facts. Clearly, more evidences are needed to *test this hypothesis*.

Except for HA basalt, another explanation for the distinct geochemical characteristics of this region is lateral impact mixing. On the  $\text{TiO}_2$  abundance map derived from Wide Angle Camera <sup>[13]</sup>, it is obvious that the ejecta derived from Finsen crater covers the eastern part of Von Kármán crater floor. In Fig. 1, we notice Apollo 15 soil and regolith breccias falls in CE-4 chemical domain. Apollo 15 soils contain 4 chemical components: mare basalt, KREEP basalt, pyroclastic green glass and highland materials <sup>[14]</sup>.

Apparently, CE-4 landing site is contaminated with the ejecta from surrounding craters. The materials in this area could be the mixture of local mare basalt, mafic ejecta from Finsen crater, highland materials

from Alder crater and others Th-rich materials from Oresme V crater. Low-Ti basalt and Finsen ejecta (Ca/Fe-rich pyroxene) are the two most significant components of the regolith in the CE-4 landing site (Fig. 2).

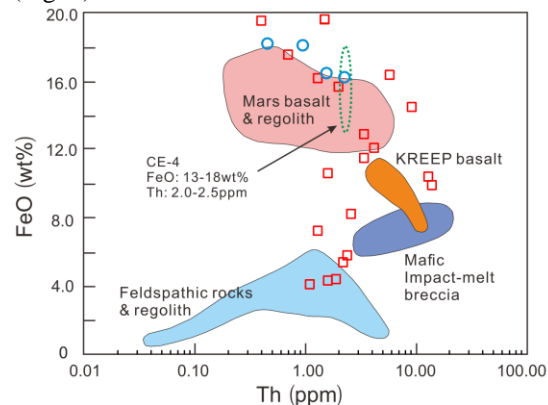


**Fig. 2** Variations of FeO and Th in lunar rock, soil and regolith samples. The Th-FeO diagram shows the different lunar rock domains. This plot is modified from [15-16]. Apollo and Luna soils chemical data (red squares) are derived from [17]. Blue circles represent Apollo 14 HA basalts [7].

**Dark haloed craters and their implication for the landing site subsurface structure:** On the Moon, the young lunar craters are usually surrounded by bright ejecta patterns or high reflectance ray system, due to the excavation of fresh, high-albedo material from beneath the mature deposits. The existence of dark-rayed /dark haloed craters (DHC) has long been noted. They are interpreted as the excavation of low albedo material from subsurface. The presence of DHCs has been taken as the indicator of ancient lunar volcanic deposits or cryptomaria<sup>[18]</sup>.

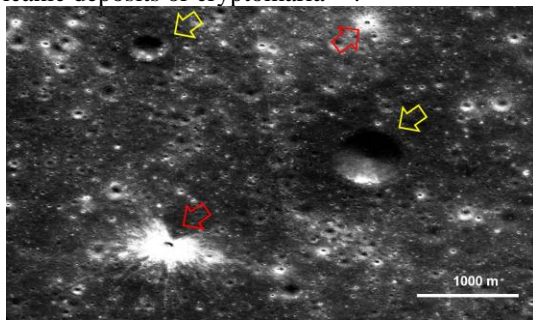


**Fig. 3** DHCs on the eastern floor of Von Kármán crater. Yellow arrows show two DHCs. Two small craters with bright rays have also been noted (red arrows).

Using LROC NAC images with solar incidence angle between 40 and 55 degrees, 16 DHCs have been identified in the eastern region of Von Kármán crater (Fig. 3). This confirmed our above observation that the continuous ejecta blanket from Finsen crater deposits on the mare basalt plain. Most of these DHCs are small crater with the diameter less than 1 km. The DHCs size and distribution on the floor could help constrain the subsurface structure of CE-4 landing site.

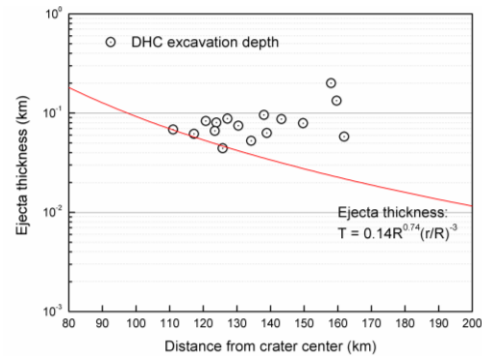


**Fig. 4** Distribution of Finsen ejecta within Von Kármán crater. Ejecta thickness (red curve) was calculated using the model of [19]. The radius of Finsen crater (R) is 36 km.

We collected the diameters of 16 DHCs and their distances (r) from Finsen crater center. The ejecta Thickness (T) was calculated using the equation of [19]. The excavation depth of each crater was calculated with the equation  $D_{exc} = D \cdot 0.1^{[20]}$ . Note all DHCs circles lie on or above the ejecta thickness curve (Fig. 4). This suggests the two layers structure in CE-4 landing site: Finsen ejecta and low-Ti basalt. The McGetchin model could be used to determine the thickness upper limit of Finsen ejecta distributed in Von Kármán. In future, we plan to search more DHCs and bright craters (not penetrate Finsen ejecta) to constrain subsurface structure of CE-4 landing site, and perform a mineralogic survey for these craters using the M<sup>3</sup> reflectance data. These works will provide valuable information about the structures and the mineral compositions of CE-4 stratigraphy.

**Acknowledgement:** This study is supported by the China NSF (41490633 and 41590851). Special thanks to LROC QuickMap, a convenient and user-friendly tool.

**References:** [1] Jolliff B.L. et al. (2000) *JGR*, 105, 4197-4216. [2] Jolliff B.L. et al. (2010) *AGU Fall Meeting*, #P43A-01. [3] Moriarty D. P. and Pieters C. M. (2017) *JGR*, 123, 729-747. [4] Ling Z. C. et al., (2019) *50th LPSC*. [5] Hagerty J. J. et al. (2011) *JGR*, 116, E06001. [6] Kramer G. Y. (2008) *JGR*, 113, E01002. [7] Neal C. R. and Kramer G. Y., (2006) *AM.*, 91, 1521-1535. [8] Papanastassiou D. A. and Wasserburg G. J. (1972) *EPSL*, 13, 368-374. [9] Ziegler R. A. et al. (2006) *MPS.*, 41, 263-284. [10] Haskin L. and Warren P. (1991) Cambridge University Press. [11] Ling Z.C. et al., (2015) *Nat. Commun.*, 8880. [12] Huang J. (2018) *JGR*, 123, 1684-1700. [13] Sato H. et al., *Icarus*, 296, 216-238. [14] Korotev R. L. (1987) *JGR*, 92. [15] Korotev R. L. (1998) *JGR*, 103. [16] Chevrel S. D. (2002) *JGR*, 107, 5132. [17] Lucey P. (2006) *RMG*, 60, 83-219. [18] Whitten J. and Head J. W. (2015) *PSS*, 67-81. [19] McGetchin T. R. et al. (1973) *EPSL*, 20, 226-236. [20] Melosh H. J. (1989) Oxford University Press.